Systematic study of charge form factors of elastic electron-nucleus scattering with the relativistic eikonal approximation

Zaijun Wang[1,*] and Zhongzhou Ren[1,2]
[1]*Department of Physics, Nanjing University, Nanjing 210008, China*
[2]*Center of Theoretical Nuclear Physics, National Laboratory of Heavy-Ion Accelerator at Lanzhou, Lanzhou 730000, China*
(Received 4 November 2004; published 31 May 2005)

We systematically investigate the elastic electron scattering on both stable and unstable nuclei with the relativistic eikonal approximation, where the charge density distributions of nuclei are from the self-consistent relativistic mean field model. Calculations show that the relativistic eikonal approximation can reproduce the experimental data of electron scattering on nuclei ranging from the light region, such as ^{12}C, to the heavy region, such as ^{208}Pb. This is the systematic test of the relativistic eikonal approximation for elastic electron scattering for both light and heavy nuclei. With this method, further studies are made of the variation of charge form factors along isotopic chains and the sensitivity of charge form factors to the changes of charge distribution. For isotopic chains with $Z = 20$ and 28, we find that the charge form factors vary significantly with neutron number. The charge form factors shift outward and downward when the target nucleus moves from the neutron-rich region to the proton-rich region along the isotopic chain. The significant shift shows that the charge form factor is very sensitive to a change of neutron number. If the isotopic shifts of the charge form factor are measured on the next-generation electron-nucleus collider (at RIKEN and GSI), the charge size and charge distribution can be determined for unstable nuclei. The calculations will provide a reference for future experiments.

DOI: 10.1103/PhysRevC.71.054323 PACS number(s): 25.30.Bf, 21.10.Ft, 27.30.+t, 13.40.Gp

I. INTRODUCTION

In the last 10 years, the development of radioactive-isotope (RI) beam techniques [1–3] has extended our knowledge of nuclear physics from the stable nuclei to the unstable ones near the drip lines. Both experiments with the RI beam [4–16] and calculations by various nuclear models [17–25] have shown that the structure of unstable nuclei is quite different from that of stable ones [26–29].

Nuclear charge density distributions are very important to understanding the internal structure of nuclei. For many years, electron-nucleus scattering has proven to be an excellent tool for the study of nuclear charge size and charge distribution. It has provided a large amount of valuable information concerning the charge size and charge distribution of stable nuclei [30–35]. However, for unstable nuclei, no such experimental work has been done so far. Theoretical calculations on this aspect for unstable nuclei are also very rare. Thanks to the advent and development of the RI beam technique [1–3], many studies not accessible in the past have been made possible.

Based on the new techniques for producing high-quality radioactive beams, a next-generation electron-RI beam collider is now under construction at RIKEN in Japan [36,37]. A similar collider at GSI in Germany has also been approved by the German government and will be built immediately [38,39]. In addition, a new scheme, SCRIT (self-confining RI target), will also be introduced [37]. The SCRIT scheme will provide a sufficiently high luminosity for elastic electron scattering experiments to measure the charge form factor. These new facilities and scheme will offer a unique opportunity to study the internal structure of unstable nuclei by electron scattering. One of the major subjects of these new colliders is the measurement of charge form factor for unstable nuclei. It is expected that information on the charge density distributions of unstable nuclei, such as size and diffuseness, will soon be available. Therefore, it is interesting to make a systematic theoretical study on elastic electron scattering for both stable and unstable nuclei.

To perform an accurate calculation of charge form factor, the plane-wave Born approximation (PWBA), which assumes that both the initial and final electrons are plane waves, is not adequate. The most accurate method is the exact phase-shift analysis. However, as the incident energy increases, more and more phase shifts are required and the computation turns out to be too tedious. At high energies, Glauber developed his nonrelativistic eikonal approximation for the Schrödinger equation [40]. Following Glauber's approach, a relativistic eikonal approximation for the Dirac equation was proposed by Baker [41]. This method was described for predicting the elastic scattering of the Dirac particles off a scalar potential [41]. However, we have found little calculation with this method for realistic electron scattering. Therefore, in the present work, we have systematically tested this method for various nuclei for which experimental data are available. We find that this method can be sufficiently accurate in prediction of charge form factor for both light and heavy nuclei even at large scattering angles (see Sec. III A), and it is very stable and time saving. After this, a further study is made of the variation of charge form factors along isotopic chains and the sensitivity of the charge form factor to the changes of charge distribution. We note that some research on the sensitivity of charge form factor to a change of charge distribution has been done in terms of the two-parameter Fermi model by Suda [37] to find out if the charge distribution for unstable nuclei can be measured by electron-RI beam scattering. He found that

*Electronic address: zaijunwang99@hotmail.com

the minima and maxima of the charge form factor were very sensitive to a change in the size and diffuseness parameters. Other important studies on this topic have also been made by Moya de Guerra *et al*. [42] with charge densities obtained in nonrelativistic Hartree-Fock with Skyrme forces and by Antonov *et al*. [43] with phenomenological charge densities. In the present paper, we try to study the sensitivity of charge form factor to the change of charge distribution in another way. We explore the sensitivity of the charge form factor by investigating the variation of the charge form factors along isotopic chains with charge densities from the self-consistent relativistic mean field (RMF) model.

Calculations of charge form factor require charge distributions. To calculate the charge form factors for unstable nuclei, we need a reliable model to produce the charge density distributions for unstable nuclei. Very recently, the self-consistent relativistic mean field model has received wide attention because of its successful application to both stable and unstable nuclei [44–48]. Therefore, it is interesting to combine this successful nuclear structure model with the relativistic eikonal approximation for a reliable prediction of form factors for the nuclei on isotopic chains. Ca and Ni isotopic chains are two typical isotopic chains with magic proton number. They will be the appropriate candidate nuclei for the future electron-nucleus scattering experiment. Hence, we perform our calculations on these two isotopic chains by combining the relativistic eikonal approximation with the RMF model. This will make our result more realistic and reliable, and it will serve as a good reference for the coming experiments.

This paper is organized in the following way. Section II is the formalism of the relativistic eikonal approximation for electron scattering and a brief review of the RMF model. The numerical results and discussions are presented in Sec. III A summary is given in Sec. IV.

II. FORMALISM

A. The relativistic eikonal approximation

Detailed descriptions of the nonrelativistic eikonal approximation for the Schrödinger equation can be found in the classical work by Glauber [40] and many other works [49–51]. Expressions of the relativistic eikonal approximation for ultrarelativistic electron scattering from a charge distribution can be found in Ref. [41].

The starting point of the relativistic eikonal approximation is the Dirac equation for a particle moving in a scalar potential $V(r)$ [41],

$$(\alpha \cdot \mathbf{p} + \beta m - E)\psi(\mathbf{r}) = -V(\mathbf{r})\psi(\mathbf{r}), \tag{1}$$

where E and m are energy and mass of the incident particle, respectively, and α and β are the Dirac matrices. Using Green's function method, the scattering amplitude can be expressed in the following form [41]:

$$f(\theta) = -\frac{1}{4\pi}(\alpha \cdot \mathbf{k_f} + \beta m + E)\int e^{-i\mathbf{k_f}\cdot\mathbf{r}} V(\mathbf{r})\psi(\mathbf{r}) d\mathbf{r}, \tag{2}$$

where θ is the scattering angle, and $\mathbf{k_f}$ is the outgoing momentum.

Following Glauber's approach, $\psi(\mathbf{r})$ can be assumed as the following form at high energies [41],

$$\psi(\mathbf{r}) = \varphi(\mathbf{r})u_0(\mathbf{k}_0)e^{i\mathbf{k}_0\cdot\mathbf{r}}, \tag{3}$$

where $u_0(\mathbf{k}_0)$ is the incident plane-wave spinor, $\mathbf{k}_0$ is the incident momentum, and $\varphi(\mathbf{r})$ is a slowly varying modulating function.

Under high-energy approximation, the elastic differential cross section σ and form factor $F(q)$ can be expressed as [41]

$$\sigma = \cos^2\left(\tfrac{1}{2}\theta\right)|I_1(q) + I_2(q)|^2, \tag{4}$$

and

$$|F(q)|^2 = \frac{\sigma}{\sigma_M}, \tag{5}$$

where q is the momentum transfer, σ_M is the Mott cross section. $I_1(q)$ and $I_2(q)$ are given by the integrals

$$I_1(q) = -ik\int_0^R J_0(qb)[e^{2i\chi(b)} - 1]b\,db, \tag{6}$$

$$I_2(q) = -ik\int_R^\infty J_0(qb)[e^{2i\chi(b)} - 1]b\,db, \tag{7}$$

where b is the impact parameter, R is the cutoff cylindrical radius, $k = |\mathbf{k}_0|$, and J_0 is the Bessel function. For high-energy electrons ($E \simeq k$), $\chi(b)$ can be written as [40,41]

$$\chi(b) = -\frac{1}{2}\int_{-\infty}^{\infty} V(r)\,dz, \tag{8}$$

$$r = \sqrt{b^2 + z^2}. \tag{9}$$

For the region $b > R$, since the charge density vanishes beyond R, $V(r)$ can be replaced by the Coulomb potential in this region and $\chi(b)$ can be expressed as a function of the cutoff radius R [40,41]

$$\chi(b) = -\alpha Z \ln\left(\frac{b}{R}\right). \tag{10}$$

Upon substituting Eq. (10) into Eq. (7) and carrying out the integral (details can be found in the Appendix of Ref. [41]), Eq. (7) becomes

$$I_2(q) = i\frac{k}{q^2}[-i2\alpha Z(qR)^{i2\alpha Z+1}J_0(qR)S_{-i2\alpha Z,-1}(qR) + (qR)^{i2\alpha Z+1}J_1(qR)S_{1-i2\alpha Z,0}(qR) - (qR)J_1(qR)], \tag{11}$$

where $S_{\mu\nu}(Z)$ are Lommel's functions, and J_0 and J_1 are Bessel functions. For large R ($R \geqslant 8$ fm), the following asymptotic expansion of Lommel's functions can be used:

$$S_{\mu\nu}(Z) \simeq Z^{\mu-1}\left[1 - \frac{(\mu-1)^2 - \nu^2}{Z^2} + \frac{[(\mu-1)^2 - \nu^2][(\mu-3)^2 - \nu^2]}{Z^4} - \cdots\right]. \tag{12}$$

For the region $b < R$, $\chi(b)$ is given by [41]

$$\chi(b) = -Z\alpha \log\left(\frac{b}{R}\right) - 4\pi\alpha \int_b^R r^2 \rho(r) y\left(\frac{b}{r}\right) dr, \quad (13)$$

where

$$y(x) = \log\left[\frac{1+(1-x^2)^{\frac{1}{2}}}{x}\right] - (1-x^2)^{\frac{1}{2}}, \quad (14)$$

and $\rho(r)$ is the charge density distribution, which satisfies the following normalization relation:

$$\int \rho(r) d\mathbf{r} = Z. \quad (15)$$

Since we are concentrating on high-energy electron scattering off medium-heavy nuclei, the Coulomb attraction felt by the electrons must be taken into account. We do this with the standard method in electron scattering. That is, we replace the momentum transfer q with the effective momentum transfer

$$q_{\text{eff}} = q[1 + 1.5\,\alpha Z\hbar c/(E\,R_0)], \quad (16)$$

in our calculation, where $R_0 = 1.07A^{1/3}$ and A is the mass number of the nucleus. Another correction to our calculation is the recoil effect of the target nucleus. We take into account the recoil effect by dividing the cross section by the factor [32]

$$f_{\text{rec}} = \left(1 + \frac{2E\sin^2\frac{\theta}{2}}{Mc^2}\right). \quad (17)$$

The earlier Eqs. (1)–(15) along with the corrections (16) and (17) enable us to predict the form factors for a given charge density distribution.

B. The relativistic mean field model

Since the RMF model is a standard theory and the details can be found in many works [44–47], we only give the main elements here. The starting point of this model is an effective Lagrange density $\mathcal{L}$ for the interacting nucleons, the σ, ω, ρ mesons, and the photons,

$$\begin{aligned}\mathcal{L} = {} & \bar{\Psi}(i\gamma^\mu\partial_\mu - m)\Psi - g_\sigma\bar{\Psi}\sigma\Psi - g_\omega\bar{\Psi}\gamma^\mu\omega_\mu\Psi \\ & - g_\rho\bar{\Psi}\gamma^\mu\rho_\mu^a\tau^a\Psi + \tfrac{1}{2}\partial^\mu\sigma\partial_\mu\sigma - \tfrac{1}{2}m_\sigma^2\sigma^2 - \tfrac{1}{3}g_2\sigma^3 \\ & - \tfrac{1}{4}g_3\sigma^4 - \tfrac{1}{4}\Omega^{\mu\nu}\Omega_{\mu\nu} + \tfrac{1}{2}m_\omega^2\omega^\mu\omega_\mu + \tfrac{1}{4}c_3(\omega_\mu\omega^\mu)^2 \\ & - \tfrac{1}{4}R^{a\mu\nu}\cdot R^a_{\mu\nu} + \tfrac{1}{2}m_\rho^2\rho^{a\mu}\cdot\rho^a_\mu - \tfrac{1}{4}F^{\mu\nu}F_{\mu\nu} \\ & - e\bar{\Psi}\gamma^\mu A_\mu\tfrac{1}{2}(1-\tau^3)\Psi, \end{aligned} \quad (18)$$

with

$$\Omega^{\mu\nu} = \partial^\mu\omega^\nu - \partial^\nu\omega^\mu, \quad (19)$$

$$R^{a\mu\nu} = \partial^\mu\rho^{a\nu} - \partial^\nu\rho^{a\mu}, \quad (20)$$

$$F^{\mu\nu} = \partial^\mu A^\nu - \partial^\nu A^\mu, \quad (21)$$

where the meson fields are denoted by σ, ω_μ, and ρ_μ^a and their masses are denoted by m_σ, m_ω, and m_ρ, respectively. The nucleon field and rest mass are denoted by Ψ and m. A_μ is the photon field responsible for the electromagnetic interaction, $\alpha = 1/137$. The effective strengths of the coupling between the mesons and nucleons are, respectively, g_σ, g_ω, and g_ρ. g_2 and g_3 are the nonlinear coupling strengths of the σ meson. c_3 is the self-coupling term of the ω field. The isospin Pauli matrices are written as τ^a, τ^3 being the third component of τ^a.

Under the no-sea approximations and mean field approximations, a set of coupled equations for mesons and nucleons can be easily obtained by the variational principle [52–55]. This set of equations can be solved consistently by iterations. After a final solution is obtained, we can calculate the binding energies, root-mean-square radii of proton and neutron density distributions, and single-particle levels. The details of numerical calculations are described in Refs. [52] and [53].

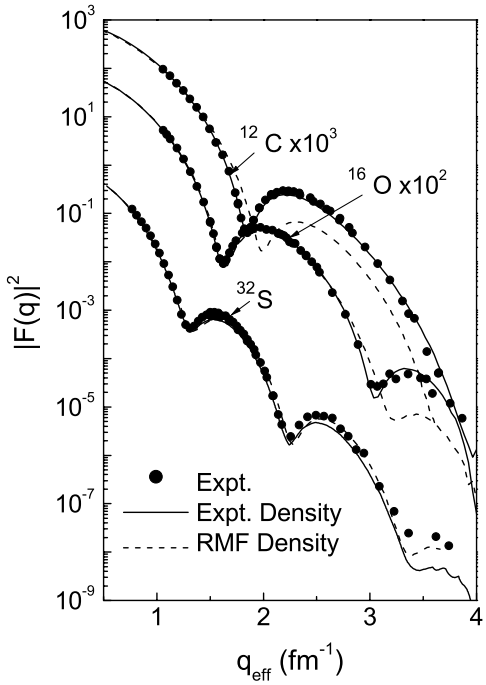

FIG. 1. Comparison of charge form factors for ^{12}C, ^{16}O, and ^{32}S. The solid and dashed lines are calculated, respectively, from the experimental charge densities [56,57] and the RMF charge densities with the relativistic eikonal approximation. The filled circles are experimental data taken from Refs. [56] and [57].

III. NUMERICAL RESULTS AND DISCUSSIONS

A. Reliability of the relativistic eikonal approximation for elastic electron-nucleus scattering

Before we proceed with calculations for isotopic chains, we need to investigate the stability and validity of the relativistic eikonal approximation. To accomplish this, we tested the relativistic eikonal approximation for various stable nuclei ranging from the light region, such as ^{12}C, to the heavy region, such as ^{208}Pb, where their experimental data are available. We give part of our testing results in Figs. 1–3.

In Fig. 1, we show comparisons of the charge form factors calculated from the experimental charge densities (the solid lines) with the experimental ones for ^{12}C, ^{16}O, and ^{32}S. The experimental charge densities are extracted by fitting the high-energy elastic electron-nucleus scattering cross sections with the exact phase-shift method [56,57]. The phase-shift

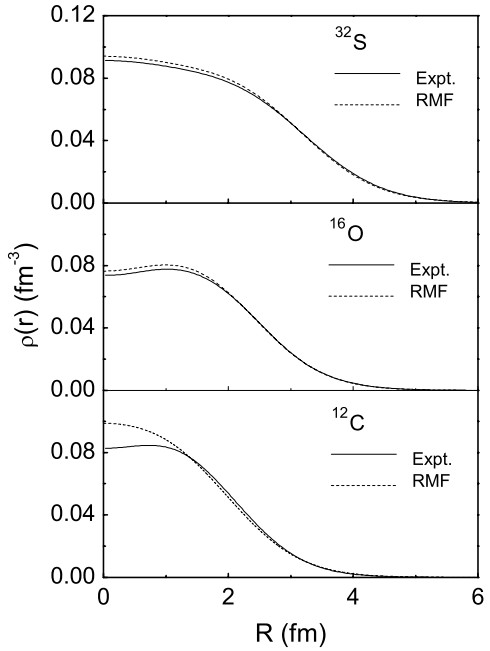

FIG. 2. Comparison of charge densities for ^{12}C, ^{16}O, and ^{32}S. The solid lines are experimental charge densities [56,57], and the dashed lines are those calculated using the RMF model.

method is based on solving the Dirac equation for the electron in the Coulomb field of the nucleus, and therefore the distortion of the electron wave and the change of the wavelength in the Coulomb field are naturally included. So it is commonly accepted that the phase-shift analysis method is the most accurate for predicting the elastic electron-nucleus scattering cross sections or form factors. When a new method is developed, it is often tested by comparing it with the method of phase-shift analysis. While the phase-shift method has its own shortcomings, the computations will become too tedious for high-energy scattering when a large number of phase shifts are calculated and the corresponding partial amplitudes with opposite signs are summed over. As described in Sec. II A, the relativistic eikonal approach is an approximation method based on the Dirac equation for high-energy elastic electron scattering. In this method, the main part of effects of the Coulomb field of the nucleus are taken into account by the introduction of the eikonal wave function [see Eq. (3)], which is obtained by a modification of the phase of the incident plane wave. For practical calculations, the other two corrections related to the change of the wavelength of the incident electrons and the recoil effect of the target nucleus should also be included [see Eqs. (16) and (17)]. From Fig. 1, we see that the experimental data [56,57] are very well reproduced by this method. The calculated magnitudes and positions of the maxima and minima agree very well with the experimental ones. This shows that the relativistic eikonal approximation can give predictions of charge form factor for nuclei with almost the same accuracy as the phase-shift analysis method. Therefore, the relativistic eikonal approximation is very accurate and reliable.

In Fig. 1, we also compared the charge form factors calculated from the RMF charge densities (the dashed lines) with the experimental ones for ^{12}C, ^{16}O, and ^{32}S. In the calculations, the NL-SH force parameters [58] are used for the RMF model. The pairing gaps for open shell nuclei are included by the Bardeen-Cooper-Schrieffer (BCS) treatment. The standard input for pairing gaps are $\Delta_n = \Delta_p = 11.2/\sqrt{A}$ MeV. The charge densities here and later are obtained by folding the point proton densities with the proton charge density distribution [59]

$$\rho_p(r) = \frac{Q^3}{8\pi} e^{-Qr}, \tag{22}$$

where $Q^2 = 18.29\ \mathrm{fm}^{-2} = 0.71\ \mathrm{GeV}^2$ ($\hbar c = 0.197$ GeV fm $= 1$). The corresponding rms charge radius is $r_p = 0.81$ fm. The contribution of neutron charge distribution to the nuclear charge form factor is neglected here, at least it is negligible at moderate momentum transfers [42,60]. It can be noted from this figure that for ^{16}O and ^{32}S, the theoretical charge form factors are in good agreement with the experimental ones except for a deviation beyond the second minimum for ^{16}O and the third minimum for ^{32}S. Whereas for ^{12}C, things are different; the theoretical results differ very much from the experimental data. These discrepancies can be explained in terms of the differences in charge density distributions. Figure 2 is an illustration of comparisons of the charge density distributions between the RMF model and the experiment. For ^{32}S and ^{16}O, the RMF charge distribution is very close to the experimental one except for a slight deviation around the center of the nucleus. This explains the deviations that occurred in the charge form factors of ^{32}S and ^{16}O (see Fig. 1), since the charge form factors at high-momentum transfers are mainly sensitive to the inner part of the charge distribution [56]. But for ^{12}C, the shapes of the RMF charge distribution and the experimental one are quite different. A slight depression appears in the experimental charge density distribution near the center, whereas in the RMF charge density distribution, the depression is replaced by a peak. Besides, another noticeable difference occurs near $r = 2$ fm in the charge distributions of ^{12}C. These differences in charge distribution between theory and experiment lead to the large discrepancy in the charge form factors of ^{12}C. But why are there such large differences in charge distribution between the RMF model and experiment for ^{12}C? We think the reason is that the RMF model is a many-body theory, and so it is not quite suitable for light nuclei such as ^{12}C. This also explains why the RMF model can give good results for the heavier nuclei like ^{16}O, ^{32}S, ^{40}Ca, ^{58}Ni, and ^{208}Pb (see Fig. 3).

Figure 3 displays the comparison of cross sections calculated from the RMF charge densities with the experimental ones for ^{40}Ca, ^{58}Ni, and ^{208}Pb. The experimental cross sections are taken from Ref. [61]. It is evident that the calculated cross sections are in good agreement with the experimental ones. Both the numbers and positions of the minima and maxima of the cross sections are accurately reproduced. The predicted magnitudes also agree with the experimental ones. For large scattering angles up to $\theta = 160^\circ$ (it corresponds to $q = 4\ \mathrm{fm}^{-1}$ at $E = 400$ MeV), the calculated cross sections are still very close to the experimental ones. These, on the one hand, show that the relativistic eikonal approximation is not only reliable

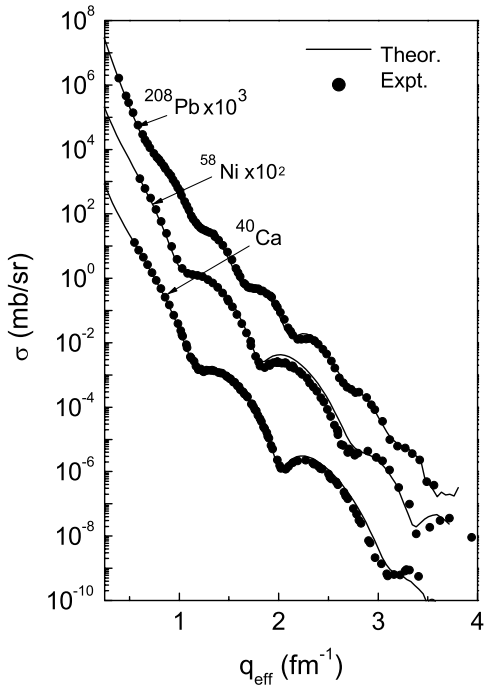

FIG. 3. Comparison of differential cross sections for scattering of 502 MeV electrons by ^{208}Pb, 449.8 Mev electrons by ^{58}Ni, and of 400 MeV electrons by ^{40}Ca. The solid lines are theoretical results from the combination of the relativistic eikonal approximation with the RMF model. The filled circles are experimental data [61].

for light nuclei but also valid for heavy nuclei, and, on the other hand, suggest that the RMF model is reliable in the prediction of charge density distributions for medium and heavy nuclei. Moreover, the good agreement between the theoretical results and the experimental ones also reveals that the neutron charge distribution does not have much influence on the charge form factors within the range of momentum transfer considered.

To sum up, we have systematically tested the relativistic eikonal approximation for elastic electron-nucleus scattering with the realistic nuclei from the light region to the heavy region. We found that this method can be accurate enough to describe the elastic electron scattering off nuclei even for heavy nuclei and at large angles. This method is also very effective and practical. Furthermore, the reliability of the RMF model in generating the charge density distributions for medium and heavy nuclei is also confirmed. In the following, we use this method to further investigate the variation of the form factors with neutron number along Ca and Ni isotopic chains and study the sensitivity of the charge form factor to the changes of charge distribution.

B. Variation of charge form factors for Ca isotopic chain

We first produce the charge densities for even Ca isotopes $^{34-60}$Ca with the RMF model. In the calculation, the NL-SH force parameters [58] are used. The pairing gaps for open shell nuclei are included by the BCS treatment. The standard input for pairing gaps are $\Delta_n = 11.2/\sqrt{A}$ MeV. For the very neutron-rich nuclei, we assume that the last neutrons just

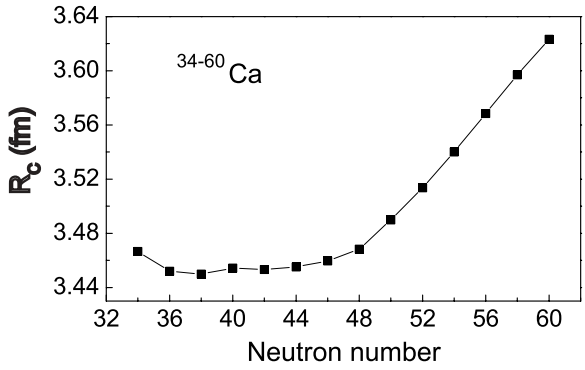

FIG. 4. Rms charge radii from the RMF model for the even Ca isotopes.

occupy the bound levels according to Tanihata [62,63]. The main results of the RMF model are presented in Figs. 4 and 5.

Figure 4 shows the calculated rms charge radii of $^{34-60}$Ca. The RMF results for ^{40}Ca and ^{48}Ca are, respectively, 3.454 and 3.468 fm. The experimental rms charge radius is 3.450 for ^{40}Ca and 3.451 fm for ^{48}Ca [35]. The deviation between the theoretical rms charge radii and the experimental ones is less than 0.02 fm. The smallest charge radii fall to the stable isotopes on or near the stability line. The charge radius becomes larger as the isotope falls far from the stability line. This indicates that the number of neutrons has significant influences on the charge size and charge distribution. In order to show the influences clearly, we plot the charge densities in Fig. 5. One can find from this figure that the charge distributions vary considerably from isotope to isotope. The variation of the charge densities on the isotopic chain has the following features. First, the densities around the center of the nuclei ($r < 3$ fm) decrease as the neutron number increases. ^{60}Ca has the lowest densities around the center and ^{34}Ca has the highest ones. Second, the spatial extension of charge distribution of the neutron-deficient isotopes is larger than that of the neutron-rich ones, although the latter has a larger rms charge radius. This can be seen clearly from the

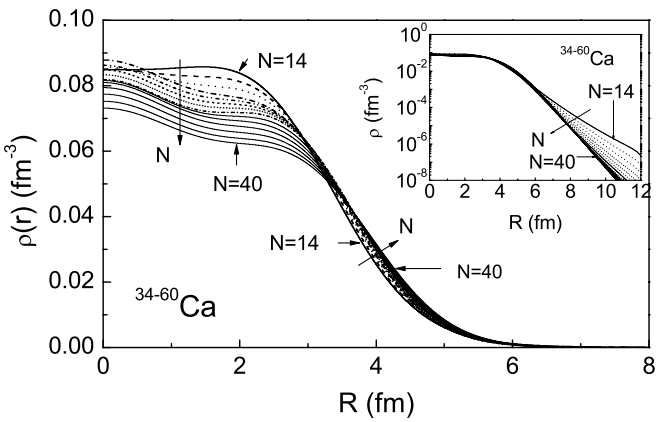

FIG. 5. Charge density variation with neutron number from the RMF model for the even Ca isotopes. The inset is in logarithmic scale. Arrows point to the directions in which the neutron number increases.

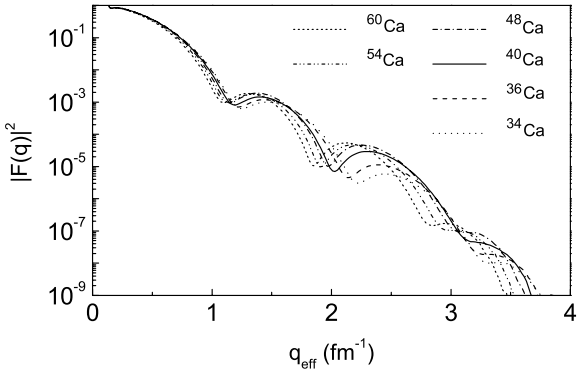

FIG. 6. The charge form factor variation with neutron number from the relativistic eikonal approximation for six Ca isotopes. The isotope effect in the charge form factors of these isotopes is clearly demonstrated.

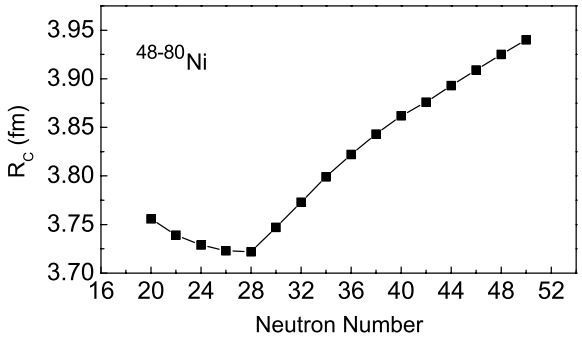

FIG. 7. Rms charge radii from the RMF model for the even Ni isotopes.

inset (in logarithmic scale) in Fig. 5. And third, it has been known that there exists a shell effect in the charge distributions of ^{40,48}Ca, since their proton numbers are magic numbers and they have closed proton shells. However, the two peaks that embody the shell effect in the charge density distribution tend to disappear as the number of neutrons decreases. This suggests that the shell effect of the charge distribution disappears for the very neutron-deficient isotopes. These features show that the isotope effect in the nuclear charge distributions of Ca isotopes is pronounced. The extreme deficiency and extreme richness in neutrons can have considerable influence on the ground-state structure of nuclei. They may lead to very different charge distributions and level structures for unstable nuclei near the drip lines.

Different charge density distributions will certainly lead to different charge form factors, since the latter is directly related to the former. So, it must be beneficial to calculate the charge form factors for the charge distributions given in Fig. 5 and study the variation of charge form factors along the isotopic chain and the sensitivity of the charge form factor to the changes of charge distribution. Fig. 6 shows the charge form factors for ^{34}Ca, ^{36}Ca, ^{40}Ca, ^{48}Ca, ^{54}Ca, and ^{60}Ca isotopes calculated by the relativistic eikonal approximation. It is seen from this figure that there are two important aspects to which we shall pay attention. One is that the charge form factors vary appreciably from isotope to isotope. This suggests that the charge form factor is very sensitive to the changes of neutron number. Compared with the charge form factors of the stable isotopes, the charge form factors of the neutron-rich ones have a considerably large inward and upward shift, and those of the neutron-deficient isotopes have a significantly large outward and downward shift. The richer or more deficient the neutrons are in an isotope, the larger is the shift of the charge form factor. The shifts of minima and maxima of the charge form factors suggest that the surface of the charge density distribution tends to become sharper when more and more neutrons are added. This implies that the diffuseness of the charge distribution is smaller for the neutron-rich isotopes than for the neutron-deficient ones. In the range of low-momentum transfer ($q < 1$ fm^{-1}), the charge form factors tend to decrease in magnitude as the neutron number increases. This can be accounted for by the following relation between the charge form factors and the rms charge radii at low-momentum transfers:

$$F(q) = 1 - \tfrac{1}{6}q^2\langle r^2\rangle + \cdots. \tag{23}$$

Therefore, in the range of low-momentum transfer, the decrease of the form factors in magnitude with the increase of the neutron number means that the rms charge radius tends to become larger as more neutrons are added. This agrees with the RMF results of the rms charge radii and charge densities shown in Figs. 4 and 5. The isotopic shifts of the rms charge radii can be determined if the charge form factors at low-momentum transfers are precisely measured. Charge form factors in the range of moderate- and high-momentum transfer are dominated by the details of the charge density distribution. The shape of the charge distribution can be determined only by measuring the form factors in this range of momentum transfer. One can find from Fig. 6 that the minima and maxima are very sensitive to the variation of neutron number. Hence, the charge form factors or the isotopic shifts of the charge form factor can be measured by electron-nucleus scattering experiments. With these data, the charge density can be extracted using the model-dependent method or the model-independent analysis (Fourier-Bessel series expansion). Another important aspect of variation of the charge form factors is the regular pattern of the isotopic shifts. It may also be useful in determining the charge form factors for an isotopic chain by experiment. Also, the regular pattern may suggest certain laws that rule the influence of neutrons on the distribution of protons. This problem deserves to be further studied.

C. Variation of charge form factors for Ni isotopic chain

With the same method and procedure used in calculations for the Ca isotopic chain, we calculated the rms charge radii, charge distributions, and the charge form factors for the Ni isotopic chain. The results are presented in Figs. 7–9.

Figure 7 represents the RMF results of the rms charge radii for the even isotopes of Ni. The figure shows that the stable isotopes have the smallest rms charge radii. The neutron-rich and neutron-deficient isotopes have a larger charge radius. The charge radius becomes even larger when more neutrons are added to or subtracted from a stable isotope. The experimental

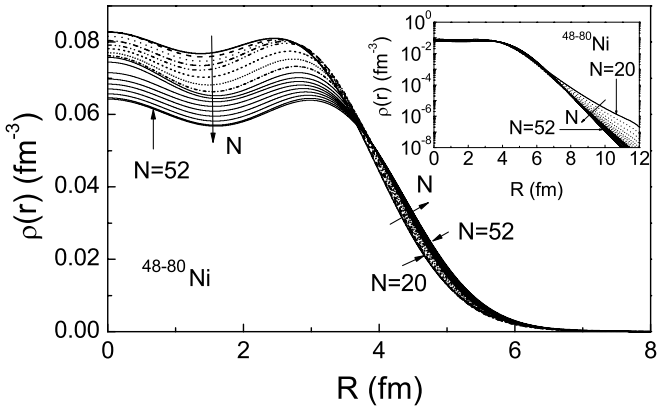

FIG. 8. Charge density variation with neutron number from the RMF model for the even Ni isotopes. The inset is in logarithmic scale. Arrows point to the directions in which the neutron number increases.

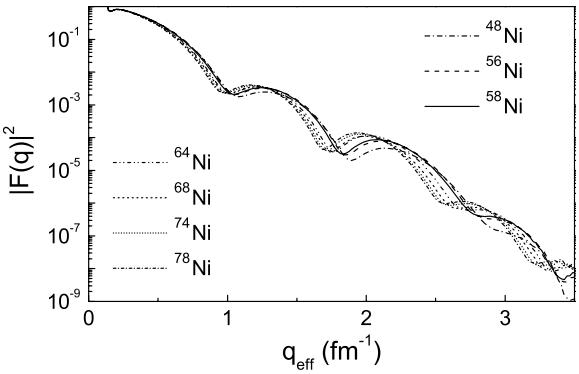

FIG. 9. Charge form factor variation with neutron number from the relativistic eikonal approximation for seven Ni isotopes. The isotope effect in the charge form factors of Ni isotopes is clearly demonstrated.

charge radius for the stable isotopes ^{58}Ni, ^{60}Ni, ^{62}Ni, and ^{64}Ni are, respectively, 3.742, 3.764, 3.802, and 3.821 fm [35]. The calculated results corresponding to the four isotopes are 3.747, 3.773, 3.799, and 3.822 fm, respectively. The deviation between the theoretical rms charge radii and the experimental ones is less than 0.02 fm. In Fig. 8, we plot the charge densities for the even isotopes of Ni. The variation of charge density distributions with neutron number is similar to that of Ca isotopes apart from two exceptions. One is that the shell effect is more pronounced for Ni isotopes than for Ca isotopes. Another is that the shell effect tends to disappear for very neutron-deficient isotopes of Ca (see Fig. 5), but still exists for very neutron-deficient Ni isotopes. These two differences may be because $Z = 28$ is a better proton shell closure than $Z = 20$, although both $Z = 28$ and $Z = 20$ are shell closures. The $Z = 20$ proton shell closure is more easily influenced by a change of neutron number than the $Z = 28$ proton shell closure. Currently, some experimental research has been done on this aspect and has shown that certain neutron magic numbers may disappear and some may exist in the very neutron-rich region [26–29]. Perhaps this phenomenon also exists for protons for the very proton-rich nuclei near the proton drip line.

Figure 9 shows the calculated charge form factors for ^{48}Ni, ^{56}Ni, ^{58}Ni, ^{64}Ni, ^{68}Ni, ^{74}Ni, and ^{78}Ni isotopes. This figure gives a full description of the variation of charge form factors with neutron number for the even isotopes of Ni. It is seen that the variation of the charge form factors of Ni isotopes is very similar to that of Ca isotopes. When the neutron number changes, the charge form factors vary significantly with a regular pattern. This suggests that the charge form factor is very sensitive to the changes of neutron number. It is expected that this isotope effect can be observed on the next-generation electron-RI beam collider. By accurately measuring the isotopic shifts of the charge form factor on an isotopic chain, the charge density distributions for the unstable nuclei can be determined.

We have, thus far, presented the theoretical calculations of charge densities and charge form factors for Ca and Ni isotopic chains based on the relativistic eikonal approximation and the RMF model. As mentioned in the Introduction, some important research on this topic has previously been done. Therefore, it would be interesting to compare the present results with the previous ones obtained for different isotopic chains with different methods. Moya de Guerra *et al.* [42] calculated the squared charge form factors as a function of momentum transfer for several Kr isotopes from the extreme proton-rich case ($A = 72$) to the highly neutron-rich region ($A = 92$) through a stable isotope ($A = 82$) with the charge densities from the deformed self-consistent mean field calculations. Their calculations showed a shift to the left (right) of the maxima and minima in the charge form factors with increasing (decreasing) neutron number, and thus the sensitivity of the form factor to the changes of the charge density with neutron number. Another study was made by Suda [37]. Using tin isotopes as an example, he discussed the sensitivities of the charge form factor to the changes of charge distribution with the two-parameter Fermi model and found that the minima and maxima have different sensitivities to a change in size and diffuseness. Very recently, the effects of a different number of neutrons on the charge density distribution of the light neutron-rich exotic nuclei were studied by Antonov *et al.* [43]. They calculated and compared the charge form factors for light exotic nuclei using various phenomenological models of charge density and pointed out that the effects of the neutron excess on the charge distribution could be tested by measuring the charge form factors with electron-nucleus scattering using a colliding electron-exotic nucleus storage ring. Thus, one can see that the present results on form factors of Ca and Ni isotopic chains obtained by combining the relativistic eikonal approximation with the RMF model supports the previous ones. Also, this discussion shows that the results on charge form factors of isotopic chains are not relevant to the models used.

IV. CONCLUSION

In summary, we performed a systematic study of the elastic electron scattering for both stable and unstable nuclei by the relativistic eikonal approximation with the charge densities from the RMF model. For stable nuclei from the light to the heavy region, the results agree very well with the available experimental data. This, on the one hand, shows that the

relativistic eikonal approximation is sufficiently accurate and reliable in description of elastic electron scattering off nuclei and, on the other hand, suggests that the charge distributions produced with the RMF model for stable nuclei are reliable. Calculations for Ca and Ni isotopic chains show that the charge form factors vary significantly and regularly with neutron number. Both maxima and minima of the charge form factor exhibit a pronounced shift when the neutron number changes, indicating that the charge form factor is very sensitive to a change in neutron number. If the isotopic shifts of the charge form factor are precisely measured by the future electron-nucleus scattering experiment, the charge size and charge distribution for unstable nuclei can be determined. Thus, it will be very interesting to measure the charge form factors on an isotopic chain by the electron-nucleus scattering experiment (at RIKEN [36,37] and GSI [38,39]). Our calculations will serve as a good reference for the coming experiments.

ACKNOWLEDGMENTS

Z. R thanks Professor W. Q. Shen, Professor H. Q. Zhang, and Professor Z. Y. Ma for discussions on electron scattering. This work is supported by the National Natural Science Foundation of China (Grant No. 10125521), the 973 National Major State Basic Research and Development of China (Grant No. G2000077400), the CAS Knowledge Innovation Project No. KJCX2-SW-N02, and the Research Fund of Higher Education under Contract No. 20010284036.

[1] I. Tanihata, Prog. Part. Nucl. Phys. **35**, 505 (1995).
[2] H. Geissel, G. Münzenberg, and K. Riisager, Annu. Rev. Nucl. Part. Sci. **45**, 163 (1995).
[3] A. Mueller, Prog. Part. Nucl. Phys. **46**, 359 (2001).
[4] I. Tanihata, H. Hamagaki, O. Hashimoto, Y. Shida, N. Yoshikawa, K. Sugimoto, O. Yamakawa, T. Kobayashi, and N. Takahashi, Phys. Rev. Lett. **55**, 2676 (1985).
[5] I. Tanihata, T. Kobayashi, O. Yamakawa, S. Shimoura, K. Ekuni, K. Sugimoto, N. Takahashi, and T. Shimoda, Phys. Lett. **B206**, 592 (1988).
[6] W. Mittig, J. M. Chouvel, Zhan Wen Long, L. Bianchi, A. Cunsolo, B. Fernandez, A. Foti, J. Gastebois, A. Gillibert, C. Gregoire, Y. Schutz, and C. Stephan Phys. Rev. Lett. **59**, 1889 (1987).
[7] T. Kobayashi, O. Yamakawa, K. Omata, K. Sugimoto, T. Shimoda, N. Takahashi, and I. Tanihata, Phys. Rev. Lett. **60**, 2599 (1988).
[8] M. G. Saint-Laurent, R. Anne, D. Bazin, D. Guillemaud-Mueller, U. Jahnke, Jin Gen Ming, A. C. Mueller, J. F. Bruandet, F. Glasser, S. Kox, E. Liatard, Tsan Ung Chan, G. J. Costa, C. Heitz, Y. El-Masri, F. Hanappe, R. Bimbot, E. Arnold, and R. Neugart, Z. Phys. A **332**, 457 (1989).
[9] T. Nilsson, F. Humbert, W. Schwab, H. Simon, M. H. Smedberg, M. Zinser, Th. Blaich, M. J. G. Borge, L. V. Chulkov, Th. W. Elze, H. Emling, H. Geissel, K. Grimm, D. Guillemaud-Mueller, P. G. Hansen, R. Holzmann, H. Irnich, B. Jonson, J. G. Keller, H. Klingler, A. A. Korsheninnikov, J. V. Kratz, R. Kulessa, D. Lambrecht, Y. Leifels, A. Magel, M. Mohar, A. C. Mueller, G. Münzenberg, F. Nickel, G. Nyman, A. Richter, K. Riisager, C. Scheidengerger, G. Schrieder, B. M. Sherrill, K. Stelzer, J. Stroth, O. Tengblad, W. Trautmann, E. Wajda, M. V. Zhukov, and E. Zude, Nucl. Phys. **A598**, 418 (1996).
[10] M. Zinser, F. Humbert, T. Nilsson, W. Schwab, Th. Blaich, M. J. G. Borge, L. V. Chulkov, H. Eickhoff, Th. W. Elze, H. Emling, B. Franzke, H. Freiesleben, H. Geissel, K. Grimm, D. Guillemaud-Mueller, P. G. Hansen, R. Holzmann, H. Irnich, B. Jonson, J. G. Keller, O. Klepper, H. Klingler, J. V. Kratz, R. Kulessa, D. Lambrecht, Y. Leifels, A. Magel, M. Mohar, A. C. Mueller, G. Münzenberg, F. Nickel, G. Nyman, A. Richter, K. Riisager, C. Scheidengerger, G. Schrieder, B. M. Sherrill, H. Simon, K. Stelzer, J. Stroth, O. Tengblad, W. Trautmann, E. Wajda, and E. Zude, Phys. Rev. Lett. **75**, 1719 (1995).
[11] N. A. Orr, N. Anantaraman, Sam M. Austin, C. A. Bertulani, K. Hanold, J. H. Kelley, D. J. Morrissey, B. M. Sherrill, G. A. Souliotis, M. Thoennessen, J. S. Winfield, and J. A. Winger, Phys. Rev. Lett. **69**, 2050 (1992).
[12] R. Anne, S. E. Arnell, R. Bimbot, H. Emling, D. Guillemaud-Mueller, P. G. Hansen, L. Johannsen, B. Jonson, M. Lewitowicz, S. Mattsson, A. C. Mueller, R. Neugart, G. Nyman, F. Pougheon, A. Richter, K. Riisager, M. G. Saint-Laurent, G. Schrieder, O. Sorlin, and K. Wilhelmsen, Phys. Lett. **B250**, 19 (1990).
[13] A. Navin, D. Bazin, B. A. Brown, B. Davids, G. Gervais, T. Glasmacher, K. Govaert, P. G. Hansen, M. Hellström, R. W. Ibbotson, V. Maddalena, B. Pritychenko, H. Scheit, B. M. Sherrill, M. Steiner, J. A. Tostevin, and J. Yurkon, Phys. Rev. Lett. **81**, 5089 (1998).
[14] R. Morlock, R. Kunz, A. Mayer, M. Jaeger, A. Müller, J. W. Hammer, P. Mohr, H. Oberhummer, G. Staudt, and V. Kölle, Phys. Rev. Lett. **79**, 3837 (1997).
[15] H. Y. Zhang, W. Q. Shen, Z. Z. Ren, Y. G. Ma, W. Z. Jiang, Z. Y. Zhu, X. Z. Cai, D. Q. Fang, C. Zhong, L. P. Yu, Y. B. Wei, W. L. Zhu, Z. Y. Guo, G. Q. Xiao, J. S. Wang, J. C. Wang, Q. J. Wang, J. X. Li, M. Wang, and Z. Q. Chen, Nucl. Phys. **A707**, 303 (2002).
[16] Z. Li, W. Liu, X. Bai, Y. Wang, G. Lian, Z. Li, and S. Zeng, Phys. Lett. **B527**, 50 (2002).
[17] Zhongzhou Ren and Gongou Xu, Phys. Lett. **B252**, 311 (1990).
[18] G. F. Bertsch and H. Esbensen, Ann. Phys. (NY) **209**, 327 (1991).
[19] M. V. Zhukov, B. V. Danilin, D. V. Fedorov, J. M. Bang, I. J. Thompson, and J. S. Vaagen, Phys. Rep. **231**, 151 (1993).
[20] P. G. Hansen, A. S. Jensen, and B. Jonson, Annu. Rev. Nucl. Part. Sci. **45**, 591 (1995).
[21] J. S. Al-Khalili, J. A. Tostevin, and I. J. Thompson, Phys. Rev. C **54**, 1843 (1996).
[22] T. Otsuka, N. Fukunishi, and H. Sagawa, Phys. Rev. Lett. **70**, 1385 (1993).
[23] Zhongzhou Ren, Baoqiu Chen, Zhongyu Ma, and Gongou Xu, Phys. Rev. C **53**, R572 (1996).
[24] B. A. Brown and P. G. Hansen, Phys. Lett. **B381**, 391 (1996).
[25] M. V. Zhukov and I. J. Thompson, Phys. Rev. C **52**, 3505 (1995).
[26] H. Iwasaki, T. Motobayashi, H. Akiyoshi, Y. Ando, N. Fukuda, H. Fujiwara, Zs. Fülöp, K. I. Hahn, Y. Higurashi, M. Hirai, I. Hisanaga, N. Iwasa, T. Kijima, T. Minemura, T. Nakamura,

M. Notani, S. Ozawa, H. Sakurai, S. Shimoura, S. Takeuchi, T. Teranishi, Y. Yanagisawa, and M. Ishihara, Phys. Lett. **B481**, 7 (2000).
[27] T. Motobayashi, Y. Ikeda, Y. Ando, K. Ieki, M. Inoue, N. Iwasa, T. Kikuchi, M. Kurokawa, S. Moriya, S. Ogawa, H. Murakami, S. Shimoura, Y. Yanagisawa, T. Nakamura, Y. watanabe, M. Ishihara, T. Teranishi, H. Okuno, and R. F. Casten, Phys. Lett. **B346**, 9 (1995).
[28] A. Ozawa, T. Kobayashi, T. Suzuki, K. Yoshida, and I. Tanihata, Phys. Rev. Lett. **84**, 5493 (2000).
[29] M. Stanoiu, F. Azaiez, Zs. Dombrádi, O. Sorlin, B. A. Brown, M. Belleguic, D. Sohler, M. G. Saint Laurent, M. J. Lopez-Jimenez, Y. E. Penionzhkevich, G. Sletten, N. L. Achouri, J. C. Angélique, F. Becker, C. Borcea, C. Bourgeois, A. Bracco, J. M. Daugas, Z. Dlouhý, C. Donzaud, J. Duprat, Zs. Fülöp, D. Guillemaud-Mueller, S. Grévy, F. Ibrahim, A. Kerek, A. Krasznahorkay, M. Lewitowicz, S. Leenhardt, S. Lukyanov, P. Mayet, S. Mandal, H. van der Marel, W. Mittig, J. Mrázek, F. Negoita, F. De Oliveira-Santos, Zs. Podolyák, F. Pougheon, M. G. Porquet, P. Roussel-Chomaz, H. Savajols, Y. Sobolev, C. Stodel, J. Timár, and A. Yamamoto, Phys. Rev. C **69**, 034312 (2004).
[30] R. Hofstadter, Rev. Mod. Phys. **28**, 214 (1956).
[31] T. W. Donnelly and J. D. Walecka, Annu. Rev. Nucl. Part. Sci. **25**, 329 (1975).
[32] T. W. Donnelly and I. Sick, Rev. Mod. Phys. **56**, 461 (1984).
[33] E. Moya de Guerra, Phys. Rep. **138**, 293 (1986).
[34] I. Sick, Prog. Part. Nucl. Phys. **47**, 245 (2001).
[35] H. De Vries, C. W. De Jager, and C. De Vries, At. Data Nucl. Data Tables **36**, 495 (1987).
[36] T. Suda, K. Maruyama, and I. Tanihata, RIKEN Accel. Prog. Rep. **34**, 49 (2001).
[37] T. Suda, in *Proceedings of the International Workshop XXXII on Gross Properties of Nuclei and Nuclear Excitations*, Hirschegg, Austria, 2004, edited by M. Buballa, J. Knoll, W. Nörenberg, B.-J. Schaefer, and J. Wambach (GSI, Darmstadt, 2004), p. 235.
[38] An international accelerator facility for beams of ions and antiprotons, GSI Report, 2002 (unpublished).
[39] H. Simon, *Proceedings of the International Workshop XXXII on Gross Properties of Nuclei and Nuclear Excitations*, Hirschegg, Austria, 2004, edited by M. Buballa, J. Knoll, W. Nörenberg, B.-J. Schaefer, and J. Wambach (GSI, Darmstadt, 2004), p. 290.
[40] R. J. Glauber, *Lectures in Theoretical Physics* (Interscience, New York, 1959), Vol. I.
[41] A. Baker, Phys. Rev. **134**, B240 (1964).
[42] E. Moya de Guerra, E. Garrido, and P. Sarriguren, in *Proceedings of the 7th International Spring Seminar on Nuclear Physics*, edited by A. Covello (World Scientific, Singapore, 2002), p. 63.
[43] A. N. Antonov, M. K. Gaidarov, D. N. Kadrev, P. E. Hodgson, and E. Moya de Guerra, Int. J. Mod. Phys. E **13**, 759 (2004).
[44] Y. K. Gambhir, P. Ring, and A. Thimet, Ann. Phys. (NY) **198**, 132 (1990).
[45] C. J. Horowitz and B. D. Serot, Nucl. Phys. **A368**, 503 (1981).
[46] Zhongyu Ma, Hualin Shi, and Baoqiu Chen, Phys. Rev. C **50**, 3170 (1994).
[47] Zhongzhou Ren, W. Mittig, and F. Sarazin, Nucl. Phys. **A652**, 250 (1999).
[48] Zhongzhou Ren, W. Mittig, Baoqiu Chen, and Zhongyu Ma, Phys. Rev. C **52**, R20 (1995).
[49] S. J. Wallace, Ann. Phys. (NY) **78**, 190 (1973).
[50] S. J. Wallace, Phys. Rev. D **9**, 406 (1974).
[51] R. G. Newton, *Scattering Theory of Waves and Particles* (McGraw-Hill, New York, 1966).
[52] P. Ring, Prog. Part. Nucl. Phys. **37**, 139 (1996).
[53] L. S. Warrier and Y. K. Gambhir, Phys. Rev. C **49**, 871 (1994).
[54] I. Tanihata, D. Hirata, T. Kobayashi, S. Shimoura, K. Sugimoto, and H. Toki, Phys. Lett. **B289**, 261 (1992).
[55] D. Hirata, H. Toki, I. Tanihata, and P. Ring, Phys. Lett. **B314**, 168 (1993).
[56] I. Sick and J. S. McCarthy, Nucl. Phys. **A150**, 631 (1970).
[57] G. C. Li, M. R. Yearian, and I. Sick, Phys. Rev. C **9**, 1861 (1974).
[58] M. M. Sharma, M. A. Nagarajian, and P. Ring, Phys. Lett. **B312**, 377 (1993).
[59] W. Greiner and J. Reinhardt, *Quantum Electrodynamics* (Springer-Verlag, Berlin Heidelberg, 1992).
[60] E. Garrido and E. Moya de Guerra, Nucl. Phys. **A650**, 387 (1999).
[61] J. M. Cavedon, Ph.D. thesis, Universite de Paris-Sud, 1980.
[62] I. Tanihata, D. Hirata, and H. Toki, Nucl. Phys. **A583**, 769 (1995).
[63] A. Ozawa, T. Kobayashi, T. Suzuki, K. Yoshida, and I. Tanihata, Phys. Rev. Lett. **84**, 5493 (2000).